Dynamics of dissociative attachment reactions in electron stimulated desorption: Cl− from condensed Cl2

R. Azria, L. Parenteau, and L. Sanche

Citation: The Journal of Chemical Physics **87**, 2292 (1987); doi: 10.1063/1.453160
View online: http://dx.doi.org/10.1063/1.453160
View Table of Contents: http://scitation.aip.org/content/aip/journal/jcp/87/4?ver=pdfcov
Published by the AIP Publishing

Dynamics of dissociative attachment reactions in electron stimulated desorption: Cl^- from condensed Cl_2

R. Azria,[a] L. Parenteau, and L. Sanche
MRC Group in Radiation Sciences, Faculté de Médecine, Université de Sherbrooke, Sherbrooke QC J1H 5N4, Canada

(Received 25 March 1987; accepted 6 May 1987)

Energy analysis of Cl^- ions produced by dissociative attachment in electron stimulated desorption from Cl_2 condensed on a platinum substrate is reported. The electron energy dependence of the Cl^- signal exhibits two peaks around 2 and 5 eV which arise, respectively, from the $^2\Pi_g$ and $^2\Pi_u$ core-excited Cl_2^-* resonant states. At higher Cl_2 coverages, a third peak is observed around 11.5 eV. From kinetic energy distributions, it is possible to ascribe this latter peak to Cl^- ions formed via the $^2\Pi_u$ resonance by electrons which have suffered energy losses through the excitation of low-lying electronic states of molecular chlorine. In the energy range of the $^2\Pi_u$ Cl_2^-* resonance, we observe that multiple scattering processes are also important and that the curve representing the kinetic energy of Cl^- ions formed via a single scattering process as a function of incident electron energy is a straight line with a slope 1/2. This indicates that the chlorine lattice is not involved in the dissociation dynamics.

I. INTRODUCTION

In this paper we report on the electron stimulated desorption (ESD) of Cl^- ions from Cl_2 molecules condensed (i.e., physisorbed) on a polycrystalline platinum substrate in the energy range 1–15 eV. Recently, ESD of negative ions has been observed from a number of condensed molecules demonstrating that the dissociative attachment (DA) process is the main mechanism responsible for producing negative ions below the energy threshold of dipolar dissociation.[1-3] In the case of oxygen,[3] it has been shown that analysis of ion energies and comparison with gas phase data are essential to identify all transient anions involved in the DA process and to understand the details of multiple scattering processes in the ESD of negative ions. In gaseous Cl_2, DA has been studied intensively[4-6] since the advent of rare gas–halogen lasers. The DA reactions

$$e + Cl_2(^1\Sigma_g^+) \rightarrow Cl_2^-* \rightarrow Cl^-(^1S) + Cl(^2P)$$

are exothermic, the dissociation limit $Cl^-(^1S) + Cl(^2P)$ lying at 1.136 eV below the ground state of molecular chlorine. According to Wigner–Witmer rules, four Cl_2^-* resonant states with symmetries $^2\Sigma_u^+$, $^2\Pi_g$, $^2\Pi_u$, and $^2\Sigma_g^+$ arise from the interaction of $Cl^-(^1S)$ and $Cl(^2P)$ fragments. The Cl^- yield shows three peaks at 0, 2.5, and 5.5 eV ascribed from angular distribution analysis[6] of these anions to the ground compound state $^2\Sigma_u^+$ and the $^2\Pi_g$ and $^2\Pi_u$ core-excited resonances, respectively. The ground electronic configuration of the chlorine molecule being (inner core) $(\sigma_g 3p)^2$ $(\pi_u 3p)^4$ $(\pi_g 3p)^4$, the $^2\Sigma_u^+$ shape resonance is formed by adding an extra electron to the lowest unfilled $(\sigma_u 3p)$ orbital. The core-excited $^2\Pi_g$ and $^2\Pi_u$ resonances are formed by exciting one electron of the $^2\Sigma_u^+$ shape resonance from the $(\pi_g 3p)$ and $(\pi_u 3p)$ to the $(\sigma_u 3p)$ orbital, respectively.

In condensed Cl_2, we find that at low coverages, the Cl^- yield in the range 1–15 eV exhibits two peaks at about 2 and 5 eV which arise from the $^2\Pi_g$ and $^2\Pi_u$ resonant states, respectively. In the energy range of this last resonance, kinetic energy (KE) distributions of Cl^- ions show structures associated with electronic excitation of chlorine molecules through multiple electron scattering. We also determine that the curve representing the KE of Cl^- ions as a function of electron energy is a straight line with a slope 1/2. We thus establish that in condensed Cl_2, the dissociation dynamics are similar to that of gaseous Cl_2; i.e., the chlorine lattice does not play a significant role in the dynamics. At high coverages, the Cl^- yield shows a third peak around 11.5 eV ascribed from KE measurements to Cl^- ions formed via the $^2\Pi_u$ Cl_2^-* resonance by electrons which have suffered energy losses through the excitation of low-lying electronic states of chlorine molecules.

II. EXPERIMENT

The apparatus is shown schematically in Fig. 1. It consists essentially of an electron gun (G), a mass spectrometer (M and D), and a closed-cycle refrigerated cryostat (C).

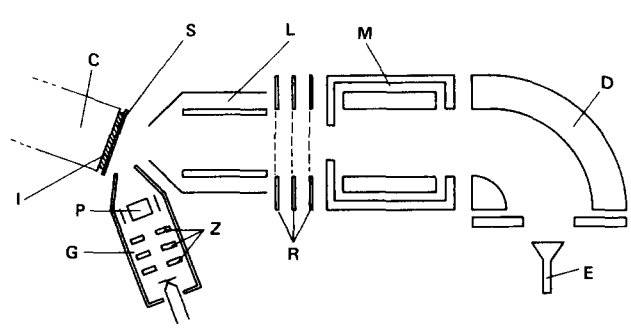

FIG. 1. Schematic diagram of electron stimulated desorption apparatus.

[a] On leave of absence from L. C. A. M. Université Paris-Sud, 91405 Orsay, France.

 0021-9606/87/162292-05$02.10

These components are housed in an ultra-high-vacuum (UHV) system reaching working pressures in the 10^{-11} Torr range. The gun (G) is composed of an indirectly heated tantalum disk which emits the electrons, a zoom lens (Z), and two perpendicular pairs of parallel deflector plates (P). The electron beam is incident at 40° from the target surface (S). It has an energy resolution of 0.3 eV full width at half-maximum (FWHM) and produces at the sample a spot of about a 2 mm^2 area above 2 eV. The beam can be scanned on S and aligned with respect to the axis of the mass spectrometer by applying proper voltages across the deflector plates (P).

The condensed films are grown on a polycrystalline platinum ribbon (S) having a surface area of 1.5×1.0 cm^2 and 0.2 mm nominal thickness. This metal substrate (S) is press fitted to the cold tip (C) of the cryostat and isolated electrically from this latter by a ceramic sheet (I). With this arrangement, it is possible to measure the electron current at the sample and clean the ribbon by resistive heating. Gases or vapors initially prepared in a UHV manifold[7] are introduced in the system through a valve connected to a tube having an opening located in front of the metal substrate (S).

A portion of the negative ions desorbed by electrons impinging on the film grown on S are focused, by the ion lens (L), at the entrance of the mass spectrometer whose axis is oriented at 70° with respect to the surface (S). Three grids (R) of about 60% transparency are placed in front of this latter in order to analyze the ion energies by the retarding potential method. The energy-discriminated ions are mass selected by a quadrupole mass filter (M), then deflected at 90° from the primary axis by a pair of cylindrical plates (D), and finally detected by a channeltron electron multiplier (E). The resulting pulses are stored in a computer as a function of electron energy or as a function of the retarding potential applied on R. The first energy derivative of this latter recording provides the energy distribution of the anions. The apparatus can therefore be operated in two modes: the ion-yield mode in which mass-selected and energy-discriminated anions are measured as a function of electron energy and the ion-energy mode in which anions of a selected mass produced at a fixed electron energy are measured as a function of the ion energy. The absolute energy scale of the electron beam is calibrated within $\pm$ 0.5 eV with respect to the vacuum level by measuring the onset of electron transmission through the films.[8] An energy resolution of 0.5 eV FWHM can be achieved in the ion-energy mode, but it is not possible to determine the absolute energy of the ions.

In the present experiment, the condensed films were prepared from Matheson reseach grade Cl_2 gas having a stated purity of 99.99%. Their thickness could be estimated within a factor of 2 from the dosing procedure previously described by Sanche.[7] With such films, spectra acquisition and energy scale calibration were particularly difficult due to the combined effects of film degradation and charging. Under electron bombardment, the film was modified by the formation of Cl and Cl^- and possibly the reaction of these latter with ground state Cl_2. Thermalized electron trapping within the film or near its surface was observed by measuring the potential created by the trapped charges. This measurement consists of monitoring the energy shift in the onset of electron transmission through the film.[8] In order to overcome problems related to degradation and charging, particularly important in the ion-energy mode, the time of data acquisition on a fresh film was kept below 3 min and the spectrum stored in the computer. We verified that during this period energy shift in the onset of transmission was smaller than the resolution of the electron beam. Afterwards, the platinum ribbon was cleaned and a new film of the same thickness was grown. This procedure was repeated 10 to 20 times for each ion KE distribution recorded at a specific incident electron energy. The different spectra thus obtained were added to provide the final energy distributions presented in this paper. The yield functions were obtained similarly. The data were recorded with incident electron currents of about 2×10^{-9} A, a target temperature of 20 K, and film thickness ranging from about 1 to 4 layers.

III. RESULTS AND DISCUSSION

The dependence of the Cl^- signal on the energy of electrons impinging on approximately one- and four-"monolayer"-thick films of condensed Cl_2 is shown at the bottom and the top of Fig. 2, respectively. The inset shows the energy dependence of the Cl^- yield in the low-energy region obtained on a monolayer film with the electron lens adjusted to transmit low-energy (1–3 eV) electrons with high efficiency. We see from these curves, that at low coverage the Cl^- yield exhibits two structures, one appearing as a shoulder around 2 eV and one as a peak around 5 eV. At higher Cl_2 coverage, another peak appears at 11.5 eV in the ion yield. Except for this later peak which cannot be assigned to a simple scattering process, there exists a relatively good agreement between the peak positions in Cl^- yields from condensed and gaseous Cl_2 in the 1–8 eV energy range. Therefore, the 2 eV and the 5 eV peaks in condensed Cl_2 are

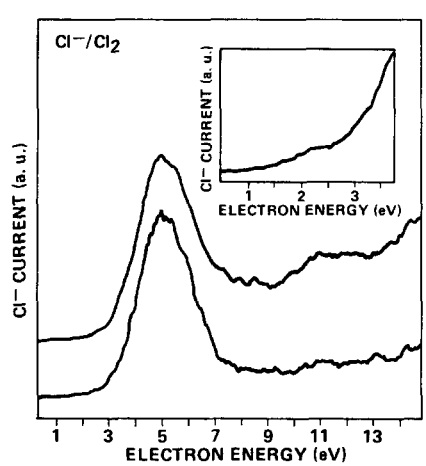

FIG. 2. The lower curve represents the energy dependence of the Cl^- yield produced by electron impact on a one-layer-thick film of condensed Cl_2. The upper curve was recorded with a four-layer-thick film. The curve in the inset was recorded on a single-layer film with the electron lens adjusted to transmit principally low-energy (1–3 eV) electrons.

ascribed, respectively, to DA processes involving the $^2\Pi_g$ and $^2\Pi_u$ Cl_2^-* core-excited resonances.

In order to understand the dissociation dynamics of Cl_2^-* ions in the solid phase and to provide a picture of electron scattering processes which lead to Cl^- ions desorption, we have recorded ion-energy spectra at different incident energies. Figure 3 shows such spectra in the energy range of the $^2\Pi_u$ Cl_2^-* resonance. These ion KE distributions exhibit structures shifting with incident energy and they are much broader than the energy resolution of the analyzing grids. Similar effects were reported for O^- ions desorption from condensed O_2 in the energy range of the $^2\Pi_u$ O_2^-* resonance.[3] When we consider the DA reaction on a diatomic molecule, i.e.,

$$e + XY \rightarrow XY^{-*} \rightarrow X^- + Y^*,$$

the excess reaction energy E is given by

$$E = E_i - (\Delta + E_n - A),$$

where Δ is the dissociation energy of the neutral molecule, A the electron affinity of X, E_i the incident electron energy, and E_n the excitation energy of the neutral fragment. This excess energy is shared between the dissociating fragments as KE. From energy and momentum conservation, the KE of the negative ion fragment is given by

$$E_r = (1-\beta)[E_i - (\Delta + E_n - A)],$$

where β is the ratio between the mass of the ion and the mass of the molecule. In the case of free homonuclear diatomic molecule β is 1/2; then, the curve representing the KE of the negative ions as a function of incident electron energy is a straight line with a slope 1/2. This is, in fact, what we observe for the high energy peak in Cl^- ions KE distributions which positions can be determined precisely as shown in Fig. 4. Therefore, the formation of these energetic Cl^- ions arise from a single scattering DA process via the $^2\Pi_u$ Cl_2^-* resonance. This result clearly indicates that no significant amount of momentum is transferred to the lattice as the Cl^- recedes from the surface. The intermolecular forces in condensed Cl_2 are therefore negligible compared to those involved in the dissociation process and the dissociation dynamics of Cl^- desorption cannot be related to the lattice of the solid. As a consequence, no appreciable phonon excitation of the lattice occurs.

According to the expression for E_r, any observation in the gas phase other than single peaks in the KE distribution at a given electron energy has to be associated with dissociating fragments in different electronic states. The first electronic excited state of Cl atoms is located above 9 eV and therefore not accessible in the energy range of the $^2\Pi_u$ Cl_2^-* resonance. Hence, the observed structure in the KE distributions of Fig. 3 must be associated with multiple scattering of incident electrons; i.e., to electrons which have suffered vibrational and electronic losses before attaching to Cl_2 molecules to form the $^2\Pi_u$ or the $^2\Pi_g$ Cl_2^-* states which dissociate. Jureta and co-workers[9] have studied threshold excitation of gaseous Cl_2 by electron impact. The yield of zero-energy electrons as a function of electron energy obtained by these authors is shown in Fig. 5 up to 8.5 eV. We see from the energy position of the excited states of Cl_2, that incoming electrons may first excite Cl_2 in the B or C electronic states and have enough residual energy to give a DA reaction via the $^2\Pi_u$ or $^2\Pi_g$ Cl_2^-* resonances. In other terms, the reaction path

$$e(E_i) + Cl_2(^1\Sigma_g^+) \rightarrow Cl_2^*(B \text{ or } C) + e(E_i - E^*)$$

followed by

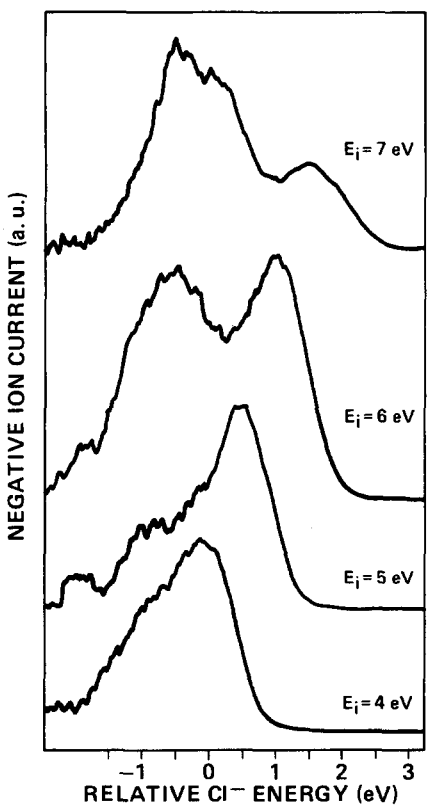

FIG. 3. Kinetic energy (KE) distribution of Cl^- ions produced by electron of energies E_i = 4, 5, 6, and 7 eV incident on a monolayer Cl_2 film. The ion energy is referenced to the maxima in the KE distribution of Cl^- ions at E_i = 4 eV.

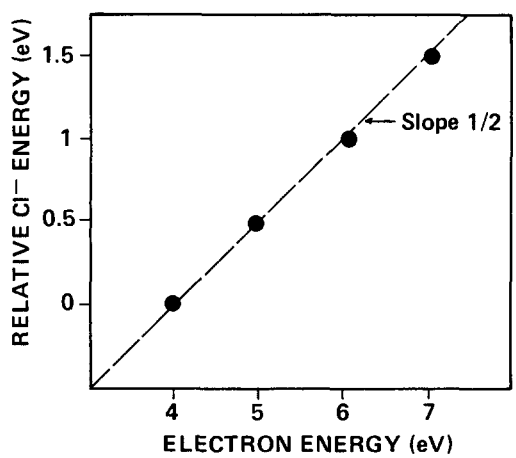

FIG. 4. KE of Cl^- ions produced from a single-layer-thick Cl_2 film vs incident electron energy E_i in the energy range of the $^2\Pi_u$ Cl_2^-* resonance.

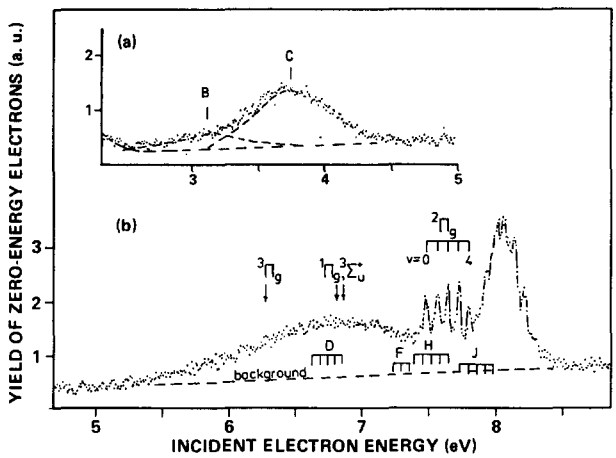

FIG. 5. Electron impact threshold spectrum of gaseous Cl_2 obtained by Jureta *et al.* (Ref. 9).

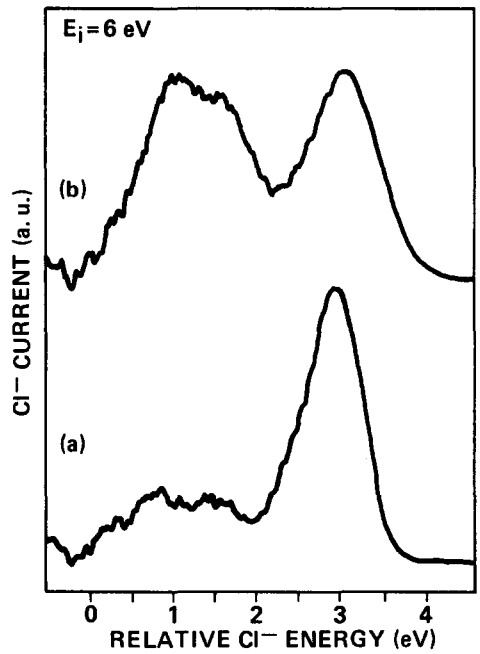

FIG. 6. KE distributions of Cl^- ions produced by 6 eV electron impact on (a) Cl_2 (0,1 monolayer)/Kr (5 layer)/Pt and (b) on Cl_2 (1 layer)/Kr (5 layer)/Pt targets.

$$e(E_i - E^*) + Cl_2(^1\Sigma_g^+) \rightarrow Cl_2^-{}^*(^2\Pi_u \text{ or } ^2\Pi_g) \rightarrow Cl^-(^1S) + Cl(^2P)$$

is energetically possible. In fact, if we consider that the *B* or *C* electronic Cl_2^* states are broad continua, the relative positions of the structures observed in the KE distributions shown in Fig. 3 agree well with the proposed mechanism assuming that Cl^- ions carry off half of the excess DA reaction energy.

These multiple scattering processes could be further evidenced by comparing the KE distributions of Cl^- ions shown in Fig. 3 with those obtained in ESD from small submonolayer coverages (i.e., $\leqslant 0.1$ monolayer). In such conditions, however, the DA reaction is influenced by the substrate, due essentially to the effects of the image charge induced in the metal.[10] These effects can be overcome if Cl_2 molecules are physisorbed on a multilayer film of rare gas condensed on the platinum ribbon.[10] Figures 6(a) and 6(b) show KE distributions of Cl^- ions produced by 6 eV electron impact from 0.1 layer of Cl_2 grown on a five-layer Kr film deposited on Pt and from a monolayer of Cl_2 deposited on such a Kr film, respectively. We see that in conditions of a very low Cl_2 coverage [Fig. 6(a)], the single scattering process leading to Cl^- ions is by far dominant. When the Cl_2 coverage increases, the multiple scattering processes become important producing the other two lower-energy structures.

Finally, we have shown in Fig. 2 that in ESD from thick Cl_2 films, a peak appears around 11.5 eV in the electron energy dependence of the Cl^- yield in addition to the two peaks at 2 and 5 eV. The KE distributions of Cl^- ions obtained in the energy range of this third peak indicate that these ions have about the same KE as those of the 5 eV peak. Consequently, we ascribe the 11.5 eV peak in the yield function to Cl^- ions formed via the $^2\Pi_u$ $Cl_2^-{}^*$ resonance by electrons which have suffered energy losses through the excitation of electronic Cl_2 states lying between about 3 and 8.5 eV.

IV. CONCLUSIONS

The formation of Cl^- ions by DA in ESD from condensed Cl_2 proceeds via the $^2\Pi_g$ and $^2\Pi_u$ $Cl_2^-{}^*$ core-excited resonances through single or multiple scattering processes involving electronic excitation of chlorine molecules. In the energy range of the $^2\Pi_u$ $Cl_2^-{}^*$ resonance, it has been possible to separate, in the KE distributions of Cl^- ions, contributions from single and multiple scattering processes. This enabled us to determine the dissociation dynamics of $Cl_2^-{}^*$ ions in the condensed phase which is found to be similar to that in the gas phase.

More generally, we can deduce from the present and previous work[1-3] that:

(i) ESD of negative ions below the dipolar dissociation threshold takes place via DA processes. The transient anions having purely repulsive potential energy curves are formed near the energy of the peaks observed in the ion yields or at a lower energy when multiple scattering processes are involved.

(ii) The KE distributions of negative ions provide insight into the electron energy degradation processes within the film and at its surface. In the case of condensed Cl_2, electronic losses are dominant, whereas in the case of solid O_2, vibrational energy losses[3] are the main multiple scattering events in the energy range of the $^2\Pi_u$ O_2^- resonance. In order to understand the dissociation dynamics of transient anions and to determine the extent of intermolecular interactions in the condensed phase, it is necessary to separate contributions from single and multiple scattering processes in the KE distributions of the desorbed ions, a measurement which can be performed easily only when vibrational losses do not control the inelastic scattering cross section.

ACKNOWLEDGMENTS

The authors wish to thank M. Michaud for helpful suggestions and critical evaluation of this manuscript. They are also indebted to J.-P. Corbeil for his valuable technical assistance. This work was supported by the Medical Research Council of Canada.

[1]L. Sanche, Phys. Rev. Lett. **53**, 1638 (1984); L. Sanche and L. Parenteau, J. Vac. Sci. Technol. A **4**, 1240 (1986).

[2]For a review of the processes leading to negative ion formation by electron impact on molecules or atoms chemisorbed on surfaces see N. H. Tolk, M. M. Traum, J. C. Tully, and T. E. Madey, *Desorption Induced by Electronic Transitions* (Springer, New York, 1983).

[3]R. Azria, L. Parenteau, and L. Sanche (to be published).

[4]M. V. Kurepa and D. S. Belic, Chem. Phys. Lett. **49**, 608 (1977).

[5]Wing-Cheung Tom and S. F. Wong, J. Chem. Phys. **68**, 5626 (1978).

[6]R. Azria, R. Abouaf, and D. T. Billy, J. Phys. B **15**, L569 (1982).

[7]L. Sanche, J. Chem. Phys. **71**, 4860 (1979).

[8]L. Sanche, G. Bader, and L. G. Caron, J. Chem. Phys. **76**, 4016 (1982).

[9]J. Jureta, S. Cvejanovic, M. Kurepa, and D. Cvejanovic, Z. Phys. A **304**, 143 (1982).

[10]H. Sambe, D. E. Ramaker, L. Sanche, and L. Parenteau (to be published).